

Antiferromagnetic Potts and Ashkin-Teller models in three dimensions

Jayanth R. Banavar

Bell Laboratories, Murray Hill, New Jersey 07974

Gary S. Grest*

Department of Physics, Purdue University, West Lafayette, Indiana 47907

David Jasnow

Department of Physics and Astronomy, University of Pittsburgh, Pittsburgh, Pennsylvania 15260

(Received 20 November 1981)

Monte Carlo simulations and renormalization-group ideas are used to analyze the behavior of the antiferromagnetic Potts model and the Ashkin-Teller model in three dimensions. A variety of continuous transitions, observed in the Monte Carlo data on the antiferromagnetic Potts model for simple cubic and body-centered-cubic lattices, are found to be consistent with ϵ -expansion analyses of these models. A glassy "plastic crystal" phase is observed, along with the analog of the glass transition in the four-state antiferromagnetic Potts model. An ϵ -expansion analysis of the Ashkin-Teller model is found to yield results consistent with those obtained by Ditzian *et al.* using series analysis and Monte Carlo simulations.

I. INTRODUCTION

There has been considerable recent work on the phase transition of the Potts model.¹ The ferromagnetic (F) case has been well studied¹⁻⁴ and it is now believed that the q -state F Potts model in $d=3$ for $q \geq 3$ exhibits a first-order transition.⁴ More recently, there has been a flurry of activity in the study of antiferromagnetic (AF) Potts models. Following the study of the phase diagram of the Ashkin-Teller model⁵ in three dimensions by Ditzian *et al.*,⁶ the four-state AF Potts model being a special case of the Ashkin-Teller model, Berker and Kadanoff⁷ studied the AF Potts model using the Migdal approximation and suggested the possibility of a novel low-temperature phase characterized by no ordering, but by algebraic decay of correlations. Subsequently, we⁸ presented the results of Monte Carlo simulations and ϵ -expansion calculations of the AF Potts model in three dimensions. More recently, further work for the AF Potts model in two dimensions has been carried out by Grest and Banavar⁹ using Monte Carlo simulations, by Cardy¹⁰ using an approximate renormalization group approach and by Nightingale and Schick¹¹ using finite size renormalization group ideas. However, the results obtained in two dimensions are not clear-cut. Studies of AF Potts models on frustrated lattices in two and three dimensions have also been reported by Grest.¹²

In this paper, we present a detailed description of results obtained by Monte Carlo and ϵ -expansion studies of AF Potts model and the Ashkin-Teller model in three dimensions. In addition to details of

the results published in our earlier letter,⁸ results for the q -state AF Potts model on a bcc lattice are presented for the first time.

We find that the Monte Carlo technique and the ϵ -expansion method, while each having their own weaknesses and strengths can be effectively used in combination to obtain a reliable picture of the phase transitions in both the AF Potts model and the Ashkin-Teller model. Our analyses suggest that the q -state AF Potts model on a simple cubic lattice with $q=3$ and 4 order at low temperatures and are in the xy and Heisenberg universality classes, respectively, whereas the AF Potts model on a bcc lattice orders for $q=3, 4$, and 5. The ϵ -expansion results suggest that if the $q=5$ AF Potts model has a continuous transition, it is characterized by cubic exponents. It is also shown that a glassy "plastic crystal" phase¹³ can be realized in the four-state AF Potts model at low temperatures. Such a phase is characterized by lack of long-range order and a lower entropy (hence higher free energy at finite temperatures) than the ordered phase. An analog of the "glass transition" is observed on heating the glassy "plastic crystal" phase. Results of ϵ -expansion studies of the Ashkin-Teller model are found to be consistent with those found using series analysis and Monte Carlo simulations by Ditzian *et al.*⁶ Further, our analysis clarifies the nature of the various transitions.

In Sec. II we describe the results of Monte Carlo simulations of the AF Potts model on a simple cubic and body-centered-cubic lattice. Section III describes the realization of a glassy "plastic crystal" phase¹³ in the Ashkin-Teller model in $d=3$ at its four-state AF

Potts point, while Sec. IV has a detailed description of the renormalization-group analysis of the AF Potts model for $q = 3, 4$, and 5 and for the Ashkin-Teller model.

II. MONTE CARLO

Our Monte Carlo (MC) calculations have been carried out on finite lattices (typically $14 \times 14 \times 14$) with periodic boundary conditions. The MC results are subject to the usual qualifications of finite sizes smearing out the transition and finite times of the simulation perhaps not leading to true equilibration. We have, however, carried out a number of runs starting from widely different starting configurations and have confirmed the equilibrium nature of the final states. All our simulations have made use of a single spin-flip sequence with both the trial spin and the final possible state of the spin being chosen at random. We also carried out simulations in which the final state of the spin was chosen at random, but where we moved sequentially through the system to locate the trial spin. Both methods gave the same results. Simulation times are measured in units of MCS/spin where 1 MCS/spin refers to each spin in the system on an average having 1 spin-flip trial (regardless of the outcome of the trial).

A. Simple cubic lattice

The AF Potts models are described by the Hamiltonian

$$-\frac{H}{kT} = -\frac{J}{kT} \sum_{\langle ij \rangle} \delta_{S_i, S_j}, \quad J < 0, \quad (2.1)$$

where $S_i = a, b, c, \dots$ is in one of q states, δ_{S_i, S_j} is the Kronecker δ function and the sum is over pairs of nearest-neighbor spins. The hypercubic lattice can be divided into two sublattices so that a site on one sublattice has its nearest-neighbor sites on the other sublattice. To determine the ground state, we started with the q states of the Potts spins assigned randomly on the lattice sites (corresponding to $T = \infty$) and lowered the temperature in small steps allowing the system to equilibrate at each temperature. The system acquired a spontaneous staggered magnetization below T_c and ordered "antiferromagnetically." For the four-state Potts model, the ordering can be visualized as having two of the four states distributed randomly on one sublattice and the other two states distributed randomly on the other sublattice. This type of ordering leads to a ground-state entropy per site of $\ln 2$. Similarly, for the three-state Potts model, a simplified view of the ordering has one of the states on the first sublattice and the other two states distributed randomly on the other sublattice leading to a ground-state entropy per site of $\frac{1}{2} \ln 2$.

We find, however, that the system does not completely order in the above fashion. On occasion, states of the Potts spins are on the "wrong" sublattice if the surrounding neighbors permit it. This leads to an *unsaturated* magnetic ordering even at zero temperature. Our results indicate that the ordering, while having a very high degeneracy, does *not* seem to have the high degree of complexity needed for the arguments of Berker and Kadanoff.⁷ The algebraic order in the low-temperature phase suggested by them may not be realized in AF Potts models in three dimensions, but the Monte Carlo results cannot rule it out categorically.

Monte Carlo simulations suggest continuous transitions for both the $q = 3$ and 4 cases in three dimensions. However, the possibility of very weak first-order transitions cannot be excluded.

The order parameter of the q -state AF Potts model may be defined to be⁸

$$M = \left(\left| \sum_{i \in I} \delta_{S_i, a} - \sum_{i \in II} \delta_{S_i, a} \right| + \left| \sum_{i \in I} \delta_{S_i, b} - \sum_{i \in II} \delta_{S_i, b} \right| + \dots \right) / N, \quad (2.2)$$

where a, b , and c are the q states of the Potts spin, I and II are the two sublattices, and N is the total number of spins. The dependence of the order parameter on the temperature is shown in Fig. 1. Figures 2 and 3 show plots of the internal energy and the specific heat for both the $q = 3$ and 4 cases. The cusps in the specific heat near the critical point suggest small negative values for the exponent α .

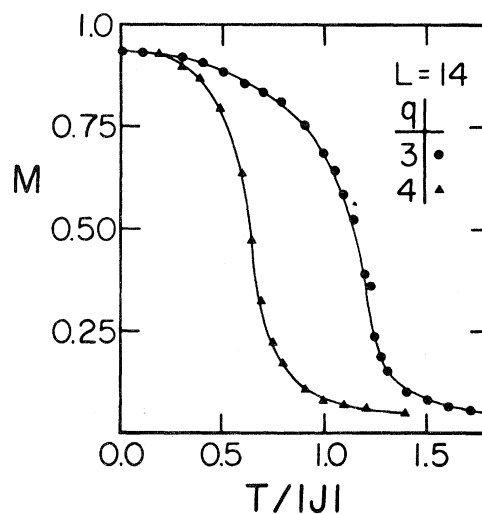


FIG. 1. The order parameter of the three- and four-state AF Potts model on a simple cubic lattice plotted as a function of the reduced temperature $T/|J|$ for a $14 \times 14 \times 14$ lattice.

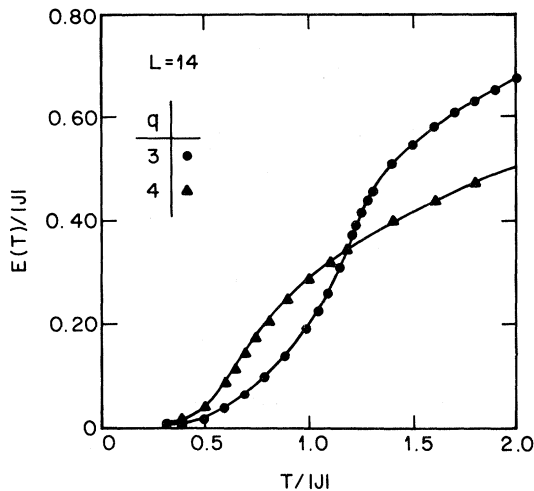


FIG. 2. Average energy vs reduced temperature for q equal to three- and four-state Potts model on a simple cubic lattice for a $14 \times 14 \times 14$ lattice.

We have also done MC simulation of the five-state AF Potts model in three dimensions. At zero temperature on a $18 \times 18 \times 18$ lattice, the order parameter M acquires a value of approximately 0.5. An analysis of the internal energy as a function of temperature, however, does not show any signal of a phase transition at finite temperatures. It seems likely, therefore, that the five-state AF Potts model on a simple cubic lattice is paramagnetic at all temperatures with the 0.5 value of the order parameter caused by finite size effects.

Figure 4 shows a plot of the order parameter M at $T=0$ as a function of q in two, three, and four dimensions. The data were taken on a 60×60 ,

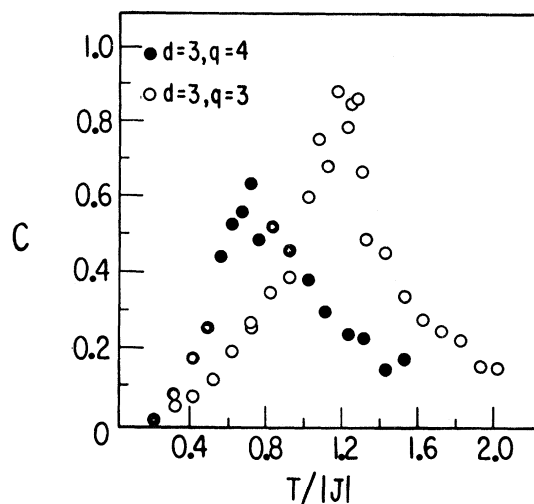


FIG. 3. Specific heats of the three- and four-state AF Potts model as a function of reduced temperature.

$18 \times 18 \times 18$, and $8 \times 8 \times 8 \times 8$ lattice in two, three, and four dimensions, respectively. The results were obtained by starting from an ordered state (corresponding to $M=1$) and running for 400 MCS/spin and averaging over the last 300. However, longer runs for $q=3, 4$, and 5 in $d=3$ were made and the results were unchanged. It is interesting to note that essentially the same results were obtained for the cases ($d=3, q=4$) and ($d=2, q=3$) for smaller lattices ($10 \times 10 \times 10$ and 36×36 , respectively), both by cooling slowly from $T > T_c$ and by starting in a perfectly ordered state at $T=0$ suggesting that the ordering is not a finite-size effect. Figure 4 shows that the magnetization is *unsaturated* even at zero temperature, as states of the Potts spins are on the “wrong” sublattice if the surrounding neighbors permit it. This becomes less likely as d increases and therefore M approaches unity as d increases. From these results, we also see that as d increases $T_c \neq 0$ for larger values of q . For $d=2, q=2$ is the only case where low-temperature order is possible, however for $d=3, q=3$ and 4 are also ordered. For $d=5, q=3, 4, 5$, and 6 appear to have $T_c \neq 0$, while T_c probably vanishes for $q \geq 7$.

We also studied the Ashkin-Teller model, for which the four-state Potts model is a special case. The Ashkin-Teller model can be considered to be a simple cubic lattice with two Ising spins σ and s sitting on each lattice site coupled by the Hamiltonian

$$-\frac{H}{kT} = \frac{J_2}{kT} \sum_{\langle ij \rangle} (\sigma_i \sigma_j + S_i S_j) + \frac{J_4}{kT} \sum_{\langle ij \rangle} \sigma_i \sigma_j S_i S_j, \quad (2.3a)$$

$$= K_2 \sum_{\langle ij \rangle} (\sigma_i \sigma_j + S_i S_j) + K_4 \sum_{\langle ij \rangle} \mu_i \mu_j \quad (2.3b)$$

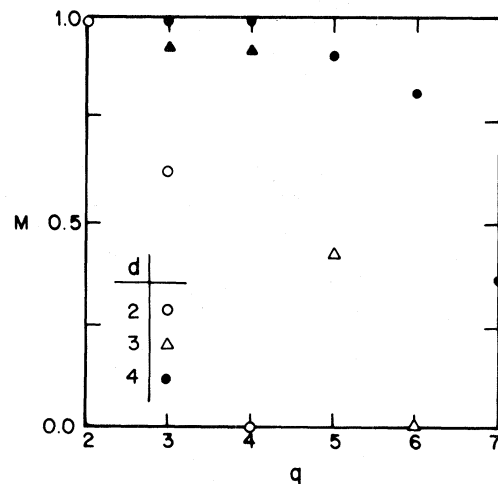


FIG. 4. The order parameter M at $T=0$ vs q for dimension $d=2, 3$, and 4 . Note that for a given q , M increases with increasing d .

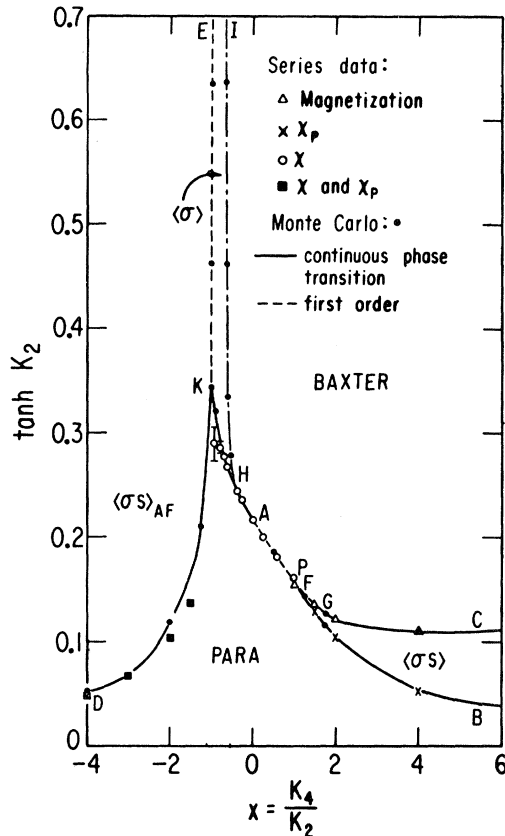


FIG. 5. Phase diagram of the Ashkin-Teller model in three dimensions obtained from series analysis and Monte Carlo simulations (from Ref. 6). The Baxter phase has $\langle \sigma \rangle$, $\langle S \rangle$, and $\langle \sigma S \rangle$ nonzero. The Baxter phase has $\langle \sigma \rangle$, $\langle S \rangle$, and $\langle \sigma S \rangle$ nonzero. The $\langle \sigma S \rangle$ and $\langle \sigma S \rangle_{AF}$ phases have the $\langle \sigma S \rangle$ product ordered ferromagnetically and antiferromagnetically, respectively, whereas the σ and S spins are disordered. In the $\langle \sigma \rangle$ phase, the symmetry between the σ and S spins is broken spontaneously and only one of them is ordered ferromagnetically. The product $\langle \sigma S \rangle$ is disordered in the $\langle \sigma \rangle$ phase. G is a tricritical point, F is a critical end point, and P is the four-state F Potts point (see Ref. 6). The line HI is believed to be first order.

where $\mu_i = \sigma_i S_i$ can take on the values ± 1 and the interaction $J_2 > 0$ is chosen to be ferromagnetic. The phase diagram of the Ashkin-Teller model was recently determined with use of series analysis and Monte Carlo simulations by Ditzian *et al.*⁶ and their results are presented in Fig. 5. The case $K_2 = K_4$ corresponds to the four-state F Potts model and $K_2 = -K_4$ corresponds to the four-state AF Potts model.

B. Body-centered-cubic lattice

We have also investigated the q -state AF Potts model (with nn interactions only) on a bcc lattice. The bcc lattice may be viewed as two interpenetrating

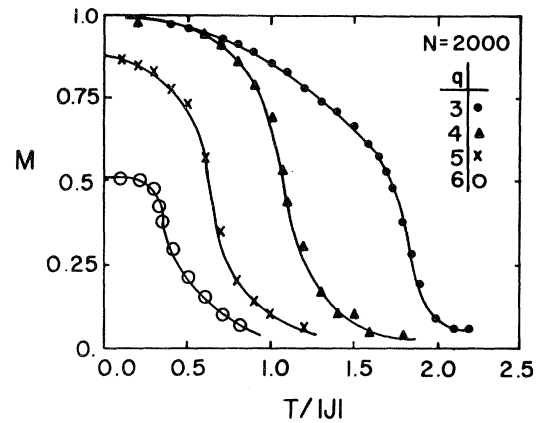


FIG. 6. The order parameter of q equal to three-, four-, and five-state AF Potts models on a bcc lattice plotted as a function of reduced temperature $T/|J|$ for a 2000-site lattice.

simple cubic lattices with each site having eight nn sites. Unlike the fcc lattice¹² and the triangular lattice¹² in two dimensions, there is no frustration in the bcc lattice. This combined with a larger coordination number than the sc lattice leads to much fewer defects in the bcc q -state AF Potts model at $T=0$ than in the corresponding sc lattice. For example, the order parameter M at $T=0$ for both the $q=3$ and 4 models on a bcc lattice is around 0.99. Another consequence of the larger coordination number in the bcc case is that the $q=5$ model clearly has a phase transition at a nonzero temperature. In this case, the low-temperature ordering may be visualized as having two of the five states distributed randomly on one of the simple cubic lattices and the other three states distributed randomly on the other simple cubic lattice.

Figures 6 and 7 show the order parameter M and the internal energy as a function of temperature for a

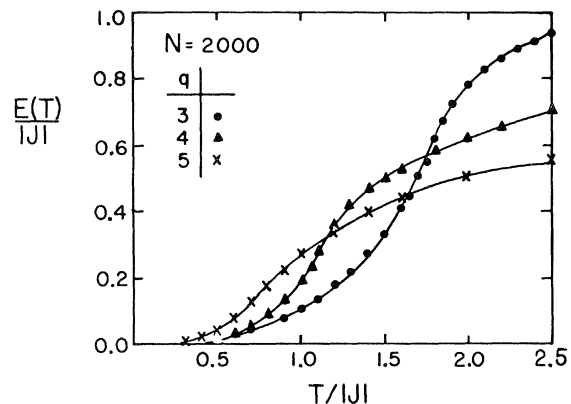


FIG. 7. Average energy vs reduced temperature for q equal to three-, four-, and five-state AF Potts models on a bcc lattice for a 2000-site lattice.

2000-site lattice for various values of q . The magnetization curve was reproducible both on heating and cooling. The $q=6$ model develops a “magnetization” of ~ 0.5 on slow cooling to zero temperature. It is unclear whether this implies a nonzero transition temperature or whether it is a finite-size effect. We find no signal of a phase transition in the internal energy and heat-capacity data, which suggests that the finite lattice is the more likely possibility. Figures 6 and 7 suggest the three-, four-, and five-state Potts models all undergo continuous transitions at a finite temperature. A weak first-order transition cannot be ruled out, however.

III. GLASSY “PLASTIC CRYSTAL” PHASE

A plastic crystal¹³ is a material which is translationally ordered and rotationally disordered at high temperatures. On cooling slowly, the molecules comprising the plastic crystal undergo rotational ordering below a characteristic melting temperature T_m . However, on quenching a plastic crystal suddenly from a temperature above T_m , it is possible to obtain a glassy plastic crystal phase in which the molecules are frozen in a state with no long-range rotational order. On heating such a glassy plastic crystal, a transition analogous to the glass transition is observed. The glassy phase is a state with higher internal energy than the equilibrium ordered phase but can be stuck in a metastable situation for very long periods of time because of internal energy barriers inhibiting rotation ordering.

The three- and four-state AF Potts models on a sc lattice order in the low-temperature phase. It is possible, however, to realize a glassy “plastic crystal” phase¹³ in the four-state AF Potts model or its Ashkin-Teller analog ($K_4 = -K_2$) by quenching suddenly to zero temperature from the paramagnetic phase. It is convenient to consider the Ashkin-Teller model since the order parameter M is unambiguous and is given by either $\langle \sigma \rangle$, $\langle S \rangle$, or $\langle \sigma S \rangle_{AF}$. The Ashkin-Teller model ($K_4 = K_2$) was quenched from a random state (corresponding to $T = \infty$) to $T = 0$ ($kT_c/J_2 = 2.9$). We then did a random search and attempted to flip either S , σ , or σS at each site to lower the internal energy. In most cases, the system reached a ground state with energy $E = -3J_2$ after about 40 MCS/spin. It was possible, however, to continue flipping some of the spins even after reaching the ground state without changing the internal energy. Attempts at flipping only S and σ after quenching from the random state resulted in the system being unable to reach a ground state after hundreds of passes through the lattice.

A number of such glassy ground states were constructed starting each time with a different random configuration at high temperature ($T \gg T_c$) and a different random number sequence. In a few cases,

the system was found to acquire a nonzero value (above the noise level) of $\langle \sigma \rangle$, $\langle S \rangle$, or $\langle \sigma S \rangle_{AF}$ in the first 40–50 MCS/spin after the quench, while approaching the ground state. These runs were not used in our studies of the time dependence of the order parameter as equilibrium was approached. Instead, we used only those glassy states in which all of the three order parameters had a value less than 0.15. The glassy “plastic crystal” states at $T = 0$ were then raised to various temperatures $T < T_c$ ($kT_c \approx 2.9J_2$) in order to study the “plastic crystal” glass transition and the time dependence of the decay to the ordered state.

Figures 8 and 9 show the time evolution of the order parameter M in two typical cases on heating to various temperatures below T_c . The order parameter M corresponds to either $\langle \sigma \rangle$, $\langle S \rangle$, or $\langle \sigma S \rangle_{AF}$ depending on which one happens to grow fastest. It is not necessary to specify which one of the three orders, since a simple change of variable maps one into the other. On raising the temperature of the zero temperature glassy phase to $T \geq 0.8J_2$, the system becomes ordered after only approximately 300 MCS/spin. This time is substantially independent of temperature for $T \geq 0.8J_2$. However, when T is raised only to $0.7J_2$, the time necessary to obtain order increases to approximately 1000 MCS/spin, as seen in curve (e) of Fig. 8 and curve (c) of Fig. 9. When the final temperature is raised to just $0.6J_2$, the system takes ~ 1500 – 2000 MCS/spin to obtain order. For a lower final temperature $T \leq 0.5J_2$, the system does not order in our observation time (~ 3000 MCS/spin). Curve (d) of Fig. 9 shows the time evolution of $\langle \sigma \rangle$, $\langle S \rangle$, and $\langle \sigma S \rangle_{AF}$ on heating

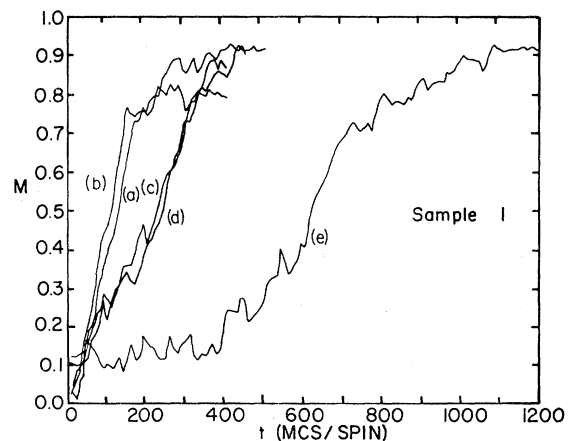


FIG. 8. Time evolution of the order parameter M on heating one of the zero-temperature glassy states (Sample 1) from $T = 0$ to (a) $T/J_2 = 2.0$, (b) 1.5, (c) 1.0, (d) 0.8, and (e) 0.7 on a $14 \times 14 \times 14$ lattice. For these temperatures, M quickly reached its equilibrium value obtained from slow cooling.

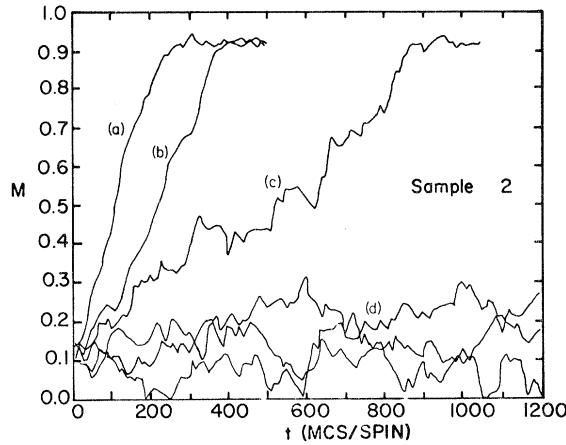


FIG. 9. Time evolution of the order parameter M on heating a second glassy state (Sample 2) from $T=0$ to (a) $T/J_2=1.0$, (b) 0.8, (c) 0.7, and (d) 0.5 on a $14 \times 14 \times 14$ lattice. For case (d), all three order parameters $\langle \sigma \rangle$, $\langle S \rangle$, and $\langle \sigma S \rangle_{AF}$ are shown. Though these fluctuate significantly, ordering does not occur, even for runs up to 3000 MCS/spin.

to $0.5 J_2$. Even though each one sometimes acquires an instantaneous value of up to 0.3, significant ordering does not set in. For all of the glassy states studied, raising to $T \leq 0.5 J_2$ left the system in a glassy state. However, raising $T \geq 0.6 J_2$ always produced ordering within our maximum observation time of ~ 3000 MCS/spin.

These unusual properties of AF Potts models may be related to the fact that domain walls in such models do not cost any internal energy. However, their construction entails a loss of entropy proportional to the area of the domain walls. It seems likely that, in the Ashkin-Teller model at $K_4 = -K_2$, the nature of the glassy phase is not associated with any topological disorder but with internal energy barriers leading to very long equilibration times at very low temperatures. In particular, it is possible that a multi-spin-flip MC sequence will lead to a more rapid decay of metastable states facilitated by the motion of domain walls.

The three-state Potts model is not a good glass former in $d=3$. When the system was quenched from $T = \infty$ to 0, after only a few hundred passes through the lattice, the system always acquired a well-defined "antiferromagnetic ordering" of the type described in Sec. II.

IV. RENORMALIZATION-GROUP ANALYSIS

A. Antiferromagnetic Potts models

The first step in a conventional renormalization-group analysis is the construction of an appropriate

Landau-Ginzburg-Wilson Hamiltonian. This can be done using symmetry arguments or systematically through the use of the Kac-Baker-Hubbard transformation,¹⁴ which is useful in transforming a model with discrete degrees of freedom to one with continuous degrees of freedom. The transformation relies on the identity

$$\exp\left(\frac{1}{2}xBx\right) = [\det(2\pi B)]^{-1/2} \times \int_{-\infty}^{\infty} dy \exp\left(-\frac{1}{2}yB^{-1}y + xy\right). \quad (4.1)$$

For compactness the quadratic forms have been expressed in scalar form. In applications x and y are nN component vectors with components \bar{x}_i and \bar{y}_i where $1 \leq i \leq N$ labels the lattice sites and $\bar{x}_i = (x_{i1}, \dots, x_{in})$. In that space B is a symmetric positive definite matrix.

As is well known³ the three-state Potts model ($q=3$) can be described in "spin language" in which case the spin vector \vec{s} at each site can point from the center of an equilateral triangle to one of the three vertices. With that constraint the reduced Hamiltonian for the $q=3$ Potts model can be written

$$\bar{H} = -\frac{H}{k_B T} = \sum_{\langle ij \rangle} K \vec{S}_i \cdot \vec{S}_j; \quad (4.2)$$

it is easy to see that this model is equivalent to the one given earlier.

The partition function for the $q=3$ Potts model can be expressed as

$$Z \propto \int_{-\infty}^{\infty} d^N \vec{\sigma} \exp\left(-\frac{1}{2} \vec{\sigma} \cdot \bar{K}^{-1} \cdot \vec{\sigma}\right) \prod_{i=1}^N \text{Tr}' \exp(\vec{\sigma}_i \cdot \vec{S}_i). \quad (4.3)$$

The trace in Eq. (4.3) is over the allowed values of \vec{S}_i according to the constraint described above. Hence the transformation has taken the system described by a discrete degree of freedom \vec{S}_i and replaced it by a continuous two-component vector $\vec{\sigma}_i$ controlled by a new weight function.³ The effective reduced Hamiltonian becomes

$$\bar{H} = -\frac{1}{2} \vec{\sigma} \cdot \bar{K}^{-1} \cdot \vec{\sigma} - \sum_i w(\vec{\sigma}_i), \quad (4.4)$$

where

$$e^{-w(\vec{\sigma})} = \text{Tr}' e^{-\vec{\sigma} \cdot \vec{S}}. \quad (4.5)$$

For a renormalization-group calculation near four dimensions one expands to fourth order in $\vec{\sigma}$ and finds

$$-w(\vec{\sigma}) = \frac{1}{4} (\vec{\sigma})^2 + \frac{1}{24} \sigma_x^3 - \frac{1}{8} \sigma_x \sigma_y^2 - \frac{1}{64} (\vec{\sigma}^2)^2 + \dots \quad (4.6)$$

as general symmetry arguments suggest. For the ferromagnetic model the third-order terms are responsible for driving the transition first order.¹⁵

The same analysis goes through for the $q=4$ state Potts model. In this case the original $\vec{\sigma}$ degrees of freedom are restricted to the vertices of a regular tetrahedron. The weight function for the *three-component* $\vec{\sigma}$ spins is then

$$-w(\vec{\sigma}) = \frac{1}{2}\sigma^2 - \sigma_x\sigma_y\sigma_z - \frac{1}{12}(\sigma_x^4 + \sigma_y^4 + \sigma_z^4) + \dots, \quad (4.7)$$

where terms higher than fourth order have been dropped. Once again this general structure follows from symmetry arguments, and the third-order term drives the ferromagnetic transition first order.

The new feature of the antiferromagnetic models is the additional symmetry imposed by the sublattice structure. When that is included the third order terms become "harmless" and one must examine the nature of the transition. To carry out the Kac-Baker-Hubbard transformation¹⁴ in this case, it is necessary to add to the interaction matrix \tilde{K} an amount $K_0\tilde{I}$, where K_0 is a suitable positive constant and \tilde{I} is the unit matrix and subtract a compensating constant from \bar{H} . This is to ensure that

$$\tilde{K}_0 = \tilde{K} + K_0\tilde{I} \quad (4.8)$$

is a positive definite matrix.

We consider a hypercubic system of two sublattices I and II. We formally consider this to be a lattice (say the I sites) with a basis. The quadratic form $\frac{1}{2}(\vec{\sigma}\cdot\tilde{K}_0\cdot\vec{\sigma})$ is then easily diagonalized essentially by transformation to the coordinates

$$\vec{\sigma}^\pm(k) = \frac{1}{\sqrt{2}}[\vec{\sigma}_I(q) \pm \vec{\sigma}_{II}(q)] \quad (4.9)$$

$$\begin{aligned} \bar{H}_3 = & -\frac{1}{2N} \sum_k [v_+(k)|\vec{\sigma}^+(k)|^2 + v_-(k)|\vec{\sigma}^-(k)|^2] \\ & -\frac{1}{24\sqrt{2}} \sum_R [3\sigma_x^+(\sigma_y^+)^2 + 3\sigma_x^+(\sigma_y^-)^2 + 6\sigma_x^-\sigma_y^+\sigma_y^- - (\sigma_x^+)^3 - 2\sigma_x^+(\sigma_x^-)] \\ & -\frac{1}{128} \sum_R \{ [(\vec{\sigma}^-)^2]^2 + [(\vec{\sigma}^+)^2]^2 + 6(\sigma_x^+)^2(\sigma_x^-)^2 + 6(\sigma_y^+)^2(\sigma_y^-)^2 + 2(\sigma_x^+)^2(\sigma_y^-)^2 + 2(\sigma_x^-)^2(\sigma_y^+)^2 \\ & + 8\sigma_x^+\sigma_x^-\sigma_y^+\sigma_y^- \} + \dots, \end{aligned} \quad (4.14)$$

where it should be recalled that there are two spins $\vec{\sigma}^+$ and $\vec{\sigma}^-$ associated with each lattice site R (or wave vector k). The analysis to this point is exact; the dots in (4.14) indicate terms higher than fourth order.

The standard treatment of this system near four

where

$$\vec{\sigma}_L(R) = \frac{1}{N} \sum_k \vec{\sigma}_L(k) e^{ik\cdot R}, \quad L = \text{I, II} \quad (4.10)$$

In this last relation N is the number of sites, \vec{R} is one of the sites, and k runs over the Brillouin zone of the I sublattice. The eigenvalues are just

$$\lambda_\pm(k) = K_0 \pm \hat{K}(k), \quad (4.11)$$

where $\hat{K}(k)$ is the Fourier transform of the original interaction matrix K_{ij} in (4.2). Instead of having one mode for each wave vector in the original Brillouin zone with the peak in the quadratic interactions occurring at the zone edge, the new description has two modes for each wave vector in the new zone with extrema moved to the zone center.

The three-state Potts model reduced Hamiltonian then becomes

$$\begin{aligned} \bar{H}_3 = & -\frac{1}{2N} \sum_k [v_+(k)|\vec{\sigma}^+(k)|^2 + v_-(k)|\vec{\sigma}^-(k)|^2] \\ & -\frac{1}{64} \sum_{R,L} [\vec{\sigma}_L^2(R)]^2 \\ & -\frac{1}{24} \sum_{R,L} [3\sigma_{Lx}(R)\sigma_{Ly}^2(R) - \sigma_{Lx}^3(R)] + \dots, \end{aligned} \quad (4.12)$$

where

$$\begin{aligned} v_\pm(k) &= \frac{1}{\lambda_\pm(k)} - \frac{1}{2} \\ &\approx c_\pm + e_\pm(ka)^2, \quad k \rightarrow 0, \end{aligned} \quad (4.13)$$

a being the lattice spacing. The terms involving $\vec{\sigma}_L(R)$ are easily expressed in terms of the normal coordinates $\vec{\sigma}^\pm$. The three-state Potts Hamiltonian then becomes

dimensions would proceed as follows. For $K < 0$ in (4.2), the *antiferromagnetic case*, one observes that the "mass" c_- in (4.13) is smaller than c_+ so that, as expected, the *staggered mode* $\vec{\sigma}^-$ is the critical mode. The noncritical mode $\vec{\sigma}^+$ is stabilized and in the paramagnetic phase which we consider, it can be

imagined to be integrated out. This will generate new terms involving the ordering mode $\bar{\sigma}^-$. The crucial point to notice is that no third-order terms of the type $(\sigma_x^-)^3$ or $\sigma_x^-(\sigma_y^-)^2$ are generated. If they were generated the conventional analysis would strongly suggest a first-order transition. Higher-order terms symbolized by the dots in (4.14) also do not generate such dangerous terms.

Hence for the purpose of studying the universal features of a reduced Hamiltonian like \bar{H}_3 one would be faced with a general $n=2$ model with fourth-order anisotropy. The familiar flow diagram corresponding to the model reduced Hamiltonian

$$\bar{H} = - \int_x \left\{ \frac{1}{2} [(\nabla \bar{\sigma})^2 + r (\bar{\sigma})^2] + u (\sigma_x^4 + \sigma_y^4) + v (\sigma_x)^2 (\sigma_y)^2 \right\} \quad (4.15)$$

is shown in Ref. 16. To $O(\epsilon)$ in $d=4-\epsilon$ dimensions¹⁶ an isotropic fixed point $v^* = 2u^* = O(\epsilon)$ ex-

ists, but for $v/u > 6$ the transition goes first order. Hence conventional analysis suggests that if the phase transition is continuous one expects xy -like behavior, with associated cusp in the specific heat, i.e., $C \sim t^{-\alpha}$ with¹⁷ $-0.2 \leq \alpha \leq -0.01$. This is in rough accord with the Monte Carlo data reported in Sec. II. Of course the possibility of a first-order transition exists; a complete analysis of irrelevant variables would be required. If one simply ignores all the nonordering components $\bar{\sigma}^+$ in (4.14) the resulting Hamiltonian \bar{H}_3 is *isotropic*. The isotropic fixed point has a domain of attraction; one would hope that integration over the nonordering fields and inclusion of irrelevant variables perturbatively does not move the Hamiltonian far from isotropy.

The situation with the four-state Potts model is similar. The same sublattice decomposition diagonalizes the quadratic part, and for $K < 0$ the staggered mode is again the ordering mode. The third-order term $\sigma_x \sigma_y \sigma_z$ in (4.7) becomes

$$\sum_R \sigma_{1x}(R) \sigma_{1y}(R) \sigma_{1z}(R) + \sum_R \sigma_{11x}(R) \sigma_{11y}(RR) \sigma_{11z}(R) = \frac{1}{\sqrt{2}} \sum_R (\sigma_x^+ \sigma_y^+ \sigma_z^+ + \sigma_x^+ \sigma_y^- \sigma_z^- + \sigma_y^+ \sigma_x^- \sigma_z^- + \sigma_z^+ \sigma_x^- \sigma_y^-) \quad (4.16)$$

Once again there are no terms of the form $(\sigma_x^-)^3$ or $(\sigma_x^- \sigma_y^- \sigma_x^-)$. The fourth-order part becomes

$$-\frac{1}{2} \sum_R \{ (\sigma_x^-)^4 + (\sigma_y^-)^4 + (\sigma_z^-)^4 + 6 [(\sigma_x^+)^2 (\sigma_x^-)^2 + 'y' + 'z'] + (\sigma_x^+)^4 + (\sigma_y^+)^4 + (\sigma_z^+)^4 \} \quad (4.17)$$

In this case if *all* nonordering '+' variables are simply ignored one finds that the starting effective three-component Hamiltonian is of the form

$$H = - \int_x \left\{ \frac{1}{2} [(\nabla \bar{\sigma})^2 + r \bar{\sigma}^2] + u (\sigma_x^4 + \sigma_y^4 + \sigma_z^4) \right\} \quad (4.18)$$

The flows take the starting Hamiltonian to the Ising-like tricritical point.^{15,16} In this case irrelevant variables and the general class of nonordering components must be considered carefully to determine whether the transition goes first order or to the isotropic Heisenberg ($n=3$) fixed point. The Monte Carlo data suggest the latter, from the cusplike specific heat in Fig. 3. This is a case where extreme caution is necessary: a naive lowest-order integration of the nonordering modes would suggest that the transition goes first order.

A similar analysis of the five-state Potts model leads to a $n=4$ continuous spin Hamiltonian with isotropic quadratic terms and anisotropic quartic terms. The antiferromagnetic symmetry, as in the previous cases, leads to the third-order terms becoming "harmless." The lowest order in ϵ for $n=4$, the

Heisenberg and cubic fixed points coincide with each other. An analysis suggests that the cubic fixed point, in this case, has a domain of attraction and that if the transition is continuous, it is characterized by cubic exponents. It is, of course, possible that, as in the simple cubic lattice in $d=3$, there is no phase transition at any temperature, i.e., the system can be paramagnetic at all temperatures.

B. Ashkin-Teller model

The Ashkin-Teller model, described by Hamiltonian (2.3), has exceptionally rich behavior. The phase boundaries in $d=3$ arising from Monte Carlo⁶ and high-temperature series⁶ analysis are shown in Fig. 5. One may again construct a Landau-Ginzburg-Wilson Hamiltonian from symmetry arguments or proceed systematically using the Kac-Baker transformation.¹⁴ Let us first assume that K_2 and K_4 are both positive (ferromagnetic) so that in reciprocal space, for small wave vector \bar{k} , $K_2(k) > 0$ and $K_4(k) \geq 0$. We will modify the arguments for $K_4 < 0$ (antiferromagnetic μ interaction) below. The Kac-Baker transformation yields

$$Z_{\text{AT}} \propto \int_{-\infty}^{\infty} d^N X d^N Y d^N Z \exp\left[-\frac{1}{2}(XK_2^{-1}X) - \frac{1}{2}(YK_2^{-1}Y) - \frac{1}{2}(ZK_4^{-1}Z)\right] \prod_i \text{Tr}_{S, \sigma} \exp(S_i X_i + \sigma_i Y_i + \mu_i Z_i) . \quad (4.19)$$

Hence for each site of the lattice three new continuous variables X_i , Y_i , and Z_i are introduced; the trace over the original σ_i and S_i variables yields a new weight function

$$-w(X_i, Y_i, Z_i) = \ln \frac{1}{2} [e^{Z_i} \cosh(X_i + Y_i) + e^{-Z_i} \cosh(X_i - Y_i)] . \quad (4.20)$$

For convenience redefining

$$\sqrt{2}Q_{\pm} = X \pm Y \quad (4.21)$$

for each site i , one finds to fourth order

$$-w = \frac{1}{2}(Q_+^2 + Q_-^2 + Z^2) - \frac{1}{24}(Q_+^4 + Q_-^4) - \frac{1}{12}Z^4 - \frac{1}{4}Q_+^2 Q_-^2 + \frac{1}{2}Z(Q_+^2 - Q_-^2) + \dots . \quad (4.22)$$

Note the appearance of a third-order term. The general structure of (4.22) could also be determined by various qualitative arguments.

The quadratic parts of the effective reduced Hamil-

$$\begin{aligned} \bar{H} = & - \int_{\mathcal{X}} \frac{1}{2} [(\nabla \sigma_x)^2 + (\nabla \sigma_y)^2 + (\nabla \sigma_z)^2 + r(\sigma_x^2 + \sigma_y^2) + r_z(\sigma_z)^2] \\ & - \int_{\mathcal{X}} [c_1(\sigma_x^4 + \sigma_y^4) + c_2 \sigma_x^2 \sigma_y^2 + c_3 \sigma_z^4 - c_4 \sigma_z(\sigma_x^2 - \sigma_y^2)] + \dots , \end{aligned} \quad (4.26)$$

where the initial values are $c_2 = 6c_1$, $c_3 = 2c_1$, and $c_4 = -12c_1$.

(i) *Ferromagnetic case, $K_2 \gg K_4 > 0$*

In this case the Z variable (or σ_z) is noncritical ($T_4^0 \ll T_2^0$) and can be integrated out. In (4.26) r_z is considered $O(1)$. When $K_4 = 0$ the transition is Ising-like and this is consistent with the ratio $c_2/c_1 = 6$. After simple integration over the σ_z variable one finds

$$\begin{aligned} c'_1 &= c_1 - \frac{1}{2}c_4^2 \langle |\sigma_z|^2 \rangle , \\ c'_2 &= c_2 + c_4^2 \langle |\sigma_z|^2 \rangle , \end{aligned} \quad (4.27)$$

where

$$\langle |\sigma_z|^2 \rangle = \int \frac{d^d k}{(2\pi)^d} \langle |\sigma_z(k)|^2 \rangle . \quad (4.28)$$

tonian combine, yielding

$$\begin{aligned} \bar{H} = & - \frac{1}{2N} \sum_k v_2(k) [|Q_+(k)|^2 + |Q_-(k)|^2] \\ & - \frac{1}{2N} \sum_k v_4(k) |Z(k)|^2 + \frac{1}{2} \sum_i Z(Q_+^2 - Q_-^2) \\ & - \frac{1}{24} \sum_i (Q_+^4 + Q_-^4 + 2Z^4 + 6Q_+^2 Q_-^2) , \end{aligned} \quad (4.23)$$

where

$$\begin{aligned} v_2(k) &\approx \left[\frac{T}{T_2^0} - 1 \right] + e_2(ka)^2 , \\ v_4(k) &\approx \left[\frac{T}{T_4^0} - 1 \right] + e_4(ka)^2 . \end{aligned} \quad (4.24)$$

Here we have defined

$$\begin{aligned} k_B T_2^0 &= 2dJ_2 \equiv 2d(k_B T K_2) , \\ k_B T_4^0 &= 2dJ_4 \equiv 2d(k_B T K_4) , \end{aligned} \quad (4.25)$$

so that T_2^0 and T_4^0 are reference or mean-field transition temperatures. Furthermore e_2 and e_4 are of order unity and positive. We now discuss the qualitative behavior of a model described by (4.23), which we rescale, rename variables, and write in standard form

After integration $c'_2/c'_1 > 6$, which suggests the transition has gone first order. The usual qualifications about the necessity for considering irrelevant variables should be made. For sufficiently small K_4 there is some confidence since $K_4 = 0$ is an Ising symmetry point.

(ii) *$K_4 \gg K_2 > 0$*

Suppose, now, that K_4 is very large. Then the Q_{\pm} (or σ_x, σ_y) modes will be noncritical and can be integrated out. The main effect of such integration will be the renormalization of r_z occurring at $O(c_4^2)$; there will also be a renormalization of c_3 at $O(c_4^4)$ yielding $c'_3 = c_3 - c_4^4 I$, where I is positive. Hence for large K_4 the first transition is expected to be Ising-like as suggested in Fig. 5. The transition involves ordering of σ_z , which traced back to the original Ashkin-Teller variables, implies ordering of the prod-

uct variables $\mu = S\sigma$. The reduction of c_3 suggests the possibility of a classical tricritical point, we shall return to this below.

Maintaining the situation $K_4 \gg K_2 > 0$ we go into the μ -ordered phase at least moderately far from the Ising line FB in Fig. 5. We shall then determine whether at lower temperatures s and σ ordering can set in. We stabilize the σ_z phase by writing $\sigma_z = m_z + \bar{\sigma}_z$, with $\langle \bar{\sigma}_z \rangle = 0$ and introduce this shift back into (4.26). If we are moderately far from the Ising line FB the $\bar{\sigma}_z$ fluctuations are not too important, however, the ordering breaks the rotational symmetry of the σ_x, σ_y system. One finds the quadratic terms modified to read in part

$$-\frac{1}{2} \int [(r + 2c_4 m_z) \sigma_y^2 + (r - 2c_4 m_z) \sigma_x^2] . \quad (4.29)$$

This suggests the possibility of ordering in the σ_y system, leading to the presence of a second Ising line at large K_4/K_2 . This is the line GC in Fig. 5. In the original variables the line corresponds to s and σ ordering.

(iii) Reducing K_4/K_2

We now consider the possibilities as K_4 is decreased (but remains positive). Consider the second transition line GC corresponding to σ_y ordering. Near the phase boundary we have

$$\bar{H}_{\text{eff}}(\sigma_y) = - \int_{\bar{x}} \left\{ \frac{1}{2} [(\nabla \sigma_y)^2 + (r + 2c_4 m_z) \sigma_y^2] + c'_1 \sigma_y^4 \right\} , \quad (4.30)$$

where c'_1 arises from renormalization by integration of the stabilized $\bar{\sigma}_z$ modes. To lowest order one has

$$c'_1 = c_1 - \frac{1}{2} c_4^2 \int \frac{d^d k}{(2\pi)^d} \frac{1}{(r_z + 12c_3 m_z^2 + k^2)} , \quad (4.31)$$

and a further reduction of c'_1 occurs because of the noncritical σ_x modes (i.e., by integrating out the

$c_2 \sigma_x^2 \sigma_y^2$ coupling). This suggests the possibility of a classical tricritical point, which presumably corresponds to point G in the phase diagram.

A similar analysis applies to the line FB separating the paramagnetic phase from the σ_z -ordered phase. As has been noted above, integration of the σ_x and σ_y degrees of freedom reduces the effective coupling c_3 in the effective $\bar{H}(\sigma_z)$. There could, in principle, appear a tricritical point on the line B in which case the merging of boundaries at F would be an ordinary triple point. The numerical results⁶ suggest that the line FB remains Ising-like all the way to F making the latter a critical end point. Since the reduction of c_3 appears at $O(c_4^4)$, one might expect that the appearance of a tricritical point on line FB is less likely than on FC as discussed above. Although the results would not be conclusive it is possible to make estimates, within the framework of an ϵ expansion, of the locations of the special points F and G .

(iv) Antiferromagnetic case, $K_4 < 0$

We now turn to the case $K_2 > 0$ and $K_4 < 0$. We have already noted that the point A ($K_4 = 0$), is an Ising (decoupled) point.

For negative K_4 we must add a constant to make the matrix \bar{K}_4 with elements positive definite [see (4.8) above]. Henceforth we consider \bar{K}_4 to be a positive-definite matrix. The analysis proceeds exactly as in the Potts models: the lattice must be divided into two sublattices and each of the transformed degrees of freedom X, Y , and Z will have normal and staggered components, e.g.,

$$X_{\pm} = X_I \pm X_{II} . \quad (4.32)$$

For positive K_2 and negative K_4 , the potentially ordering components are X_+ , Y_+ , and Z_- . Prior to elimination of nonordering modes but after some rescaling and renaming, the Hamiltonian becomes schematically

$$\begin{aligned} \bar{H} = & -\frac{1}{2N} \sum_{k, \alpha, p} v_{\alpha p}(k) |\alpha_p(k)|^2 - \int_{\bar{x}} [c_{10}(x_+^4 + y_+^4) + c_{20}(x_-^4 + y_-^4) + c_{30}(x_+^2 x_-^2 + y_+^2 y_-^2) + c_{40} z_+^4 + c_{50} z_-^4 + c_{60} z_+^2 z_-^2] \\ & + x [c_{70} x_+ y_+ z_+ + c_{80} z_- (x_+ y_- + x_- y_+) + c_{90} z_+ x_- y_-] , \end{aligned} \quad (4.33)$$

where $\alpha = x, y, z$, and $p = \pm$. The complexity of the interaction term arises from subjecting the weight function (4.20) to the appropriate sublattice decomposition. Note there are no third-order terms of the sort $x_+ y_+ z_-$ which contains three ordering components.

Now we imagine integrating out nonordering components. Terms of the form $x_+^2 x_-^2$ generate new x_+^4 couplings as well as modifying the propagator. More interestingly the third-order terms generate new quartic couplings: $c_{70}^2 x_+^2 y_+^2$ and $c_{80}^2 (x_+^2 z_-^2 + y_+^2 z_-^2)$. Hence we are led to a study of the following three-

component Hamiltonian written in standard form

$$\begin{aligned} \bar{H} = & -\frac{1}{2} \int_{\bar{x}} [(\nabla \sigma_x)^2 + (\nabla \sigma_y)^2 + r(\sigma_x^2 + \sigma_y^2)] \\ & -\frac{1}{2} \int_{\bar{x}} [(\nabla \sigma_z)^2 + r_z \sigma_z^2] \\ & - \int_{\bar{x}} [c_1(\sigma_x^4 + \sigma_y^4) + c_2 \sigma_z^4 - c_3 \sigma_x^2 \sigma_y^2 \\ & - c_4 \sigma_z^2(\sigma_x^2 + \sigma_y^2)] . \end{aligned} \quad (4.34)$$

(i) $|K_4| \gg K_2$

Tracing back to the original model the suggestion is that the product variables $\mu = s\sigma$ order antiferromagnetically; this corresponds to σ_z ordering in (4.34), where σ_x and σ_y remain noncritical. Here at large $|K_4|$ one expects an Ising line separating disordered and μ -ordered states. Presumably this corresponds to line DK in the phase diagram of Fig. 5.

(ii) $|K_4| \ll K_2$

Recall that $K_4 = 0$ is a decoupled Ising transition (point A on Fig. 5). If K_4 is small and *antiferromagnetic* analysis of (4.34) suggests that σ_z is noncritical and σ_x and σ_y are the ordering modes. Integration over the σ_z degrees of freedom yields a two-component effective Hamiltonian of the form (4.15). This $n = 2$ Hamiltonian has been studied in great detail.¹⁵ There is a domain of stability of the isotropic fixed point $v^* = 2u^*$ at which point XY -like exponents are found.¹⁶ This suggests that the *critical line* AH is an XY -like line having appropriate $n = 2$ exponents.

(iii) *Increasing* $|K_4|$

The effective Hamiltonian (4.15) technically speaking has a bicritical point corresponding to the symmetry $v = 2u$.¹⁶ Changing from $v \leq 2u$ to $v \geq 2u$ the nature of the ordered phase changes: in the former case the easy axes are the diagonals in spin space, while in the latter the ordering occurs along the x and y axes in spin space. This bicritical point appears even in mean-field theory where a first-order line must separate the two types of ordering. This is a somewhat uninteresting bicritical point even within the framework of renormalization group: both criti-

cal lines *and* the bicritical point itself have XY -like ($n = 2$) exponents, and the phase boundary passes smoothly through the bicritical point itself. This is a prototype example of the way in which irrelevant variables (v , when $v \approx 2u$) influence the nature of the ordered phases and the phase diagram.

This discussion leads to the identification of the point H in Fig. 5 as the bicritical point discussed above.

Continuing to increase $|K_4|$ we reach the point K at $K_4 = -K_2$. This is known from alternative analysis to be completely equivalent to the *antiferromagnetic* four-state ($q = 4$) Potts model. From our analysis on the $q = 4$ model above we expect that the point K corresponds to an isotropic Heisenberg ($n = 3$) point. From the Ashkin-Teller model viewpoint K becomes a *bicritical point* at the meeting of XY and Ising critical lines. Returning to our effective Ashkin-Teller reduced Hamiltonian (4.34) one sees that $n = 3$ behavior is possible (when the σ_x , σ_y , and σ_z components all order simultaneously). Apparently the coupling coefficients c_1 , etc., put the system in the domain of attraction of the isotropic fixed point. Note the cusplike shape of the critical lines meeting at K . The scaling predictions of Fisher and Nelson¹⁸ are expected to hold in the vicinity of K .

This concludes our analysis of the multicritical points and phase boundaries of the Ashkin-Teller model as originally determined by Monte Carlo and series expansion methods.⁶ Our aim here has been to show how the general structure determined by these techniques is consistent with that of a renormalization-group analysis. Renormalization-group ideas have allowed the identification of the multicritical points and the nature of the phase boundaries. No attempt has been made to make numerical estimates of the locations of various points and boundaries. The reverse problem of determining the specific Ashkin-Teller phase diagram from the renormalization-group analysis probably cannot be done completely unambiguously; the analysis here shows the general necessity of having the interplay between the various techniques.

ACKNOWLEDGMENTS

It is a pleasure to thank L. P. Kadanoff for many stimulating discussions. This work was supported in part by the National Science Foundation at Purdue University under Grant No. DMR-80-17758 and at the University of Pittsburgh under Grant No. DMR-80-02416.

*Present address: Exxon Research and Engineering Co.,
Linden, N.J. 07036.

- ¹R. B. Potts, Proc. Cambridge Philos. Soc. 48, 106 (1952).
- ²J. P. Straley and M. E. Fisher, J. Phys. A 6, 1310 (1973).
- ³R. K. P. Zia and D. J. Wallace, J. Phys. A 8, 1495 (1975);
R. G. Priest and T. C. Lubensky, Phys. Rev. B 13, 4159 (1976).
- ⁴H. W. J. Blote and R. H. Swendsen, Phys. Rev. Lett. 43,
799 (1979); S. J. Knak Jensen and O. G. Mouritsen, Phys.
Rev. Lett. 43, 1736 (1979).
- ⁵J. Ashkin and E. Teller, Phys. Rev. 64, 178 (1943).
- ⁶R. V. Ditzan, J. R. Banavar, G. S. Grest, and L. P. Kadanoff,
Phys. Rev. B 22, 2542 (1980).
- ⁷A. N. Berker and L. P. Kadanoff, J. Phys. A 13, L259
(1980).
- ⁸J. R. Banavar, G. S. Grest, and D. Jasnow, Phys. Rev. Lett.
45, 424 (1980).
- ⁹G. S. Grest and J. R. Banavar, Phys. Rev. Lett. 46, 1458
(1981).
- ¹⁰J. Cardy, Phys. Rev. B 24, 5128 (1981).
- ¹¹M. P. Nightingale and M. Schick, J. Phys. A 15, L39 (1982).
- ¹²G. S. Grest, J. Phys. A 14, L217 (1981).
- ¹³A "plastic crystal" phase is one in which the molecules (or
spins) are translationally ordered but rotationally disor-
dered. For details, see H. Suga and S. Seki, J. Non-Cryst.
Solids 16, 161 (1974).
- ¹⁴M. Kac, Phys. Fluids 2, 8 (1959); G. A. Baker, Phys. Rev.
126, 2071 (1962); J. Hubbard, Phys. Lett. 39A, 365
(1972).
- ¹⁵J. Rudnick, J. Phys. A 8, 1125 (1975).
- ¹⁶A. Aharony, in *Phase Transition and Critical Phenomena*,
edited by C. Domb and M. S. Green (Academic, New
York, 1976), Vol. 6.
- ¹⁷J. C. LeGuillou and J. Zinn-Justin, Phys. Rev. Lett. 39, 95
(1977).
- ¹⁸M. E. Fisher and D. R. Nelson, Phys. Rev. Lett. 32, 1350
(1974).